Original Article

Shielding analyses supporting the Lithium loop design and safety assessments in IFMIF-DONES

Gediminas Stankunas [a, *], Yuefeng Qiu [b], Francesco Saverio Nitti [c], Juan Carlos Marugán [d]

[a] Lithuanian Energy Institute, Laboratory of Nuclear Installation Safety, Kaunas, Lithuania
[b] Karlsruhe Institute of Technology, Karlsruhe, (KIT), Germany
[c] ENEA Brasimone, I-40032, Camugnano, BO, Italy
[d] Empresarios Agrupados Internacional (EAI), Madrid, Spain

ABSTRACT

The assessment of radiation fields in the lithium loop pipes and dump tank during the operation were performed for International Fusion Materials Irradiation Facility — DEMO-Oriented NEutron Source (IFMIF-DONES) in order to obtain the radiation dose-rate maps in the component surroundings. Variance reduction techniques such as weight window mesh (produced with the ADVANTG code) were applied to bring the statistical uncertainty down to a reasonable level. The biological dose was given in the study, and potential shielding optimization is suggested and more thoroughly evaluated. The MCNP Monte Carlo was used to simulate a gamma particle transport for radiation shielding purposes for the current Li Systems' design. In addition, the shielding efficiency was identified for the Impurity Control System components and the dump tank. The analysis reported in this paper takes into account the radiation decay source from and activated corrosion products (ACPs), which is created by d-Li interaction. As a consequence, the radiation (resulting from ACPs and Be-7) shielding calculations have been carried out for safety considerations.

1. Introduction

IFMIF-DONES (International Fusion Materials Irradiation Facility — DEMO-Oriented NEutron Source) is an irradiation facility based on d-Li neutron source which aims the qualification of materials at the irradiation conditions of the DEMO fusion power reactor, which is being developed in the frame of EUROfusion Power Plant and Technology (PPPT) programme. The high intensity neutron radiation produced in the liquid lithium target results in strong activations both of the inner Test Cell (TC) components and in the lithium loop, due to the transport of radioactive products. The strong decay gamma dose is important and needs to be estimated for the safety concern of workers and public, as well as the protection of electronic systems.

This paper presents the shielding analyses, which will be provided for supporting the design of the Lithium loop and safety assessment. The paper considers the radiation decay source from Be-7, which is produced by d-Li interaction. It has a half-life of 53

days and emits gamma rays with 477 keV of energy. Radiation shielding simulations has been performed for the safety concerns. Simulation geometry was created for the Lithium loop components, mainly Li containers and pipes. Gamma transport calculation was performed for the components concerned, e.g. the lithium dump tank and cold traps. The biological dose will be provided in the study, while possible shielding optimization are proposed and assessed in more details. A series of gamma transport are performed using the MCNP Monte Carlo, and radiation shielding suggestions are provided for maintenance design of the Li Systems.

2. IFMIF-DONES Impurity Control System

The Impurity Control System (ICS) is made up of a branch line to the Primary Li loop that collects a part of the lithium before purification and impurity analysis and then re-injects it [1]. The system is designed to condition lithium after maintenance and regulate to maintain a set level of purity prior to start-up. Cold traps, hydrogen traps, on-line impurity monitoring devices, and Li sampling devices are all found in the purification branch. Sampling units needed to quantify impurities concentration in taken lithium through a specific chemical batch analysis. The Li Purification Loop, Traps,

* Corresponding author.
  E-mail address: gediminas.stankunas@lei.lt (G. Stankunas).

Impurity Monitoring, and associated diagnostics and control are subsystems of this ICS. Since it has been shown that their presence can dramatically increase the corrosion rate exerted by the flowing metal, purification of Lithium from solved non-metals is a key element for a safe and long-lasting operation of the lithium loop; particularly, N is considered to be the most affecting one, owing to the formation of Li ternary Nitrides (Li_9CrN_5, Li_3FeN_2.) [1]. Lithium oxides might plug the cold section of the circuit at the same time. The high radioactive Tritium isotope content created by the Deuteron beam impinging on the Lithium target, on the other hand, necessitates the removal of hydrogen from the flowing metal. As a result, dissolved contaminants must be continually removed and the degree of contamination of flowing lithium must be monitored. See Figure 1.

The following functions must be performed by the ICS: 1) Keep radioactive sources like tritium (T), beryllium-7 (Be-7) and activated Activation Corrosion Products under control (ACP). 2) Control corrosion and erosion sources on structural components, such as oxygen (O), carbon (C), and nitrogen (N), while the projected N trap is an off-line trap that is incorporated in the Dump tank of the Primary Li loop. 3) Ensure liquid lithium's physical characteristics and 4) For 30 years, process impurities created in and entered into Li.

The Impurity Monitoring Loop and the Purification Loop are two sub-loops of the ICS; the first is a sampling/analysis subsystem, while the second uses Hydrogen and Cold Traps to eliminate Lithium impurities. The loop's operating temperature range is 250°C—325°C. At start-up, a bypass ratio of 0.5 percent of the nominal flow rate of the Primary Li loop is estimated to be sufficient to purify the lithium in a reasonable amount of time. 90% of the flow will pass through the traps, with the remaining 10% being sent to the monitoring loop. The flow rate through the traps should be modified on an individual basis. The flow rate through the traps should be modified on an individual basis. Lithium normally flows along both sub-loops, and regulating valves have been considered to balance the flow across the sub-loops. The flow velocity in pipe is 1.89 m/s at the necessary flow rate (0.65 l/s) [1].

The IFMIF-DONES ICS is a system that must function to control the impurities created in the Primary lithium loop. The purification loop currently has a specialized electro-magnetic pump (EMP-2) that drives Li through the purification system. The Li is removed and re-injected in the main loop's downcomer side. To minimize cavitation, the extraction position must give adequate head to the pump inlet. Valves separate the extraction and injection lines from the Primary loop. One of the Li loop's components is the Sampling unit, which is dedicated to quantify, though a specific chemical batch analysis, impurities concentration in taken lithium.

The lithium is purified during normal operation by the Li Purification Loop. The Impurity Control System is housed in R009, the "Li Trap Cell." During regular operation, Ar buffers it, and it is only available during the repair time. The Li sampler unit is put in an Ar buffered glove box in the next room, the "Li Sampling Cell" R017, under air atmosphere, in order to access it during beam operation.

2.1. Dump tank design

The Dump Tank (DT) has the following functions: 1) store and melt lithium for the initial filling and 2) during routine or emergency shutdowns, store and retain the Lithium drained. As a result, the Dump Tank is situated in a pit at the Lithium Loops' lowest elevation point. Li ingots are charged into the tank from a glove box temporarily connected to it during the installation phase. Heaters attached to the tank are used to melt Li before use and to keep the tank temperature stable during usage. The liquid Li is charged into the loop, which uses argon gas to pressurize the Dump Tank.

The total Li volume of the loop filled to the maximum level is 8.83 m^3. The capacity of the tank has been set at 12.1 m^3. Figure 2 outlines the Dump Tank's key qualities. For the pressure-resistance test, a pressure of 0.95 MPa is assumed [1].

The Nitrogen Trap is installed in the Dump Tank to lower Nitrogen (N) concentrations in lithium to less than 30 wppm; the Trap is a solid and insoluble metallic substance, known as a 'getter,' that may adsorb Nitrogen from Lithium. The Nitrogen Trap must operate at a greater temperature than the remainder of the Lithium loop (usually approximately 500—600°C). It's a big cylindrical tank where Lithium is permitted to stay in touch with the chosen getter for a long period at a high temperature. It's a big cylindrical tank where Lithium is allowed to stay in contact with the specified getter for a long period at a high temperature. After the first loading of the facility with Lithium, and after each suspension of operations for scheduled maintenance or unanticipated defects, the trap will be operated statically on the whole Lithium inventory.

3. Computational tools, data and geometry

3.1. Neutron transport calculations

Neutron transport calculations were performed by means of 3D Monte Carlo particle transport simulations with code MCNP6 [2], which is widely benchmarked and validated for fusion neutronics applications [3,4], using variety of nuclear cross-section data libraries, the specified IFMIF-DONES neutron source and the recommended geometry model(s).

Gamma flux for each TC material and water pipe cell were calculated The complete analysis was performed by means of MCNP6 with mcplib84 [2] nuclear data library. Dose maps are converted from meshtal format to VTK with dedicated scripts. CAD models can be exported into STL format. ParaView [5] visualization software allows the combination of STL geometry with VTK data.

In order to evaluate the radiological effects of the activated components, the MCNP models for DT and Li loop pipes were generated by using CAD to MCNP tool McCAD [6] developed at KIT. See Figure 3.
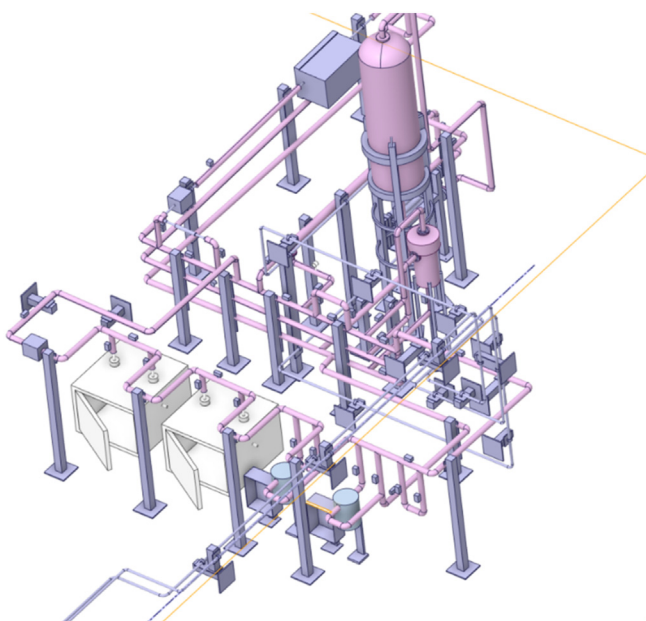

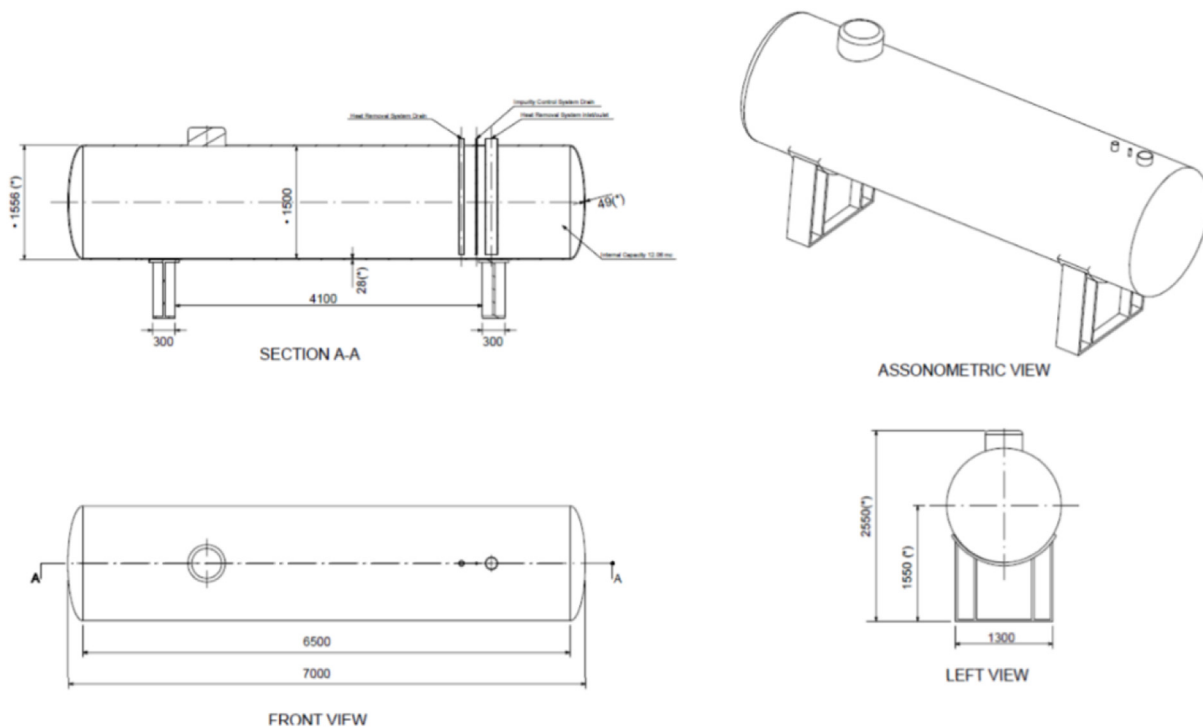**Fig. 1.** Top view of CAD model for the whole piping system with Lithium loop in R017 [1].

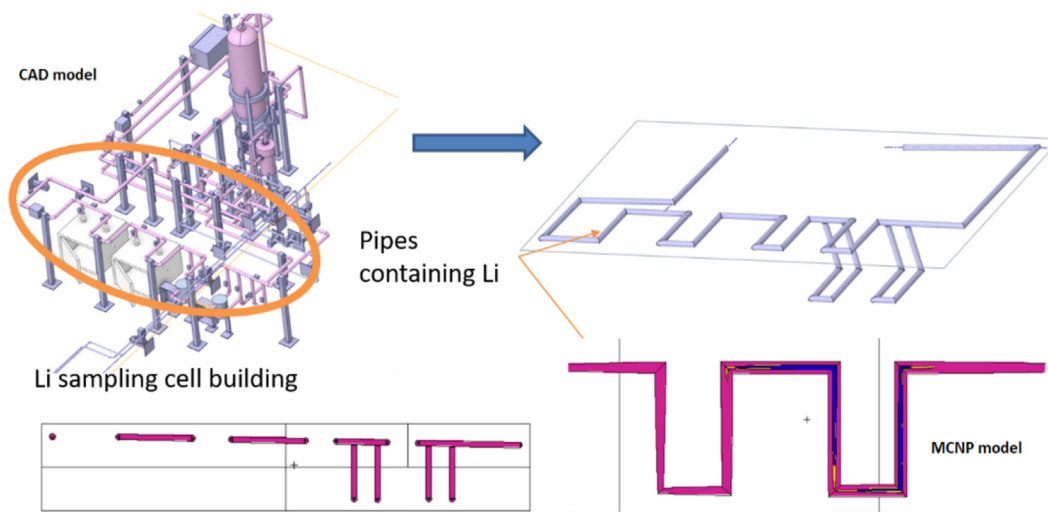**Fig. 2.** The Dump Tank's key qualities and design [1].

Fig. 3. CAD and MCNP model for Li pipes in the Li sampling cell.

3.2. Variance reduction

The AutomateD VAriaNce reducTion Generator (ADVANTG) [7] software automates the generation of variance reduction (VR) parameters for continuous-energy Monte Carlo simulations of fixed-source neutron, photon, and coupled neutron-photon transport problems using MCNP [8]. ADVANTG generates space- and energy dependent mesh-based weight-window bounds and biased source based on the three-dimensional (3-D) discrete ordinates (SN) calculations that are performed by the Denovo [9] package. The deterministic calculations can be performed using multiple cores and/or processors (e.g., on multi-core desktop systems and clusters). The final variance reduction parameters are output in a format that can be used with unmodified versions of MCNP. The primary objective of the development of ADVANTG has been to reduce both the user effort and the computational time required to obtain accurate and precise tally estimates across a broad range of challenging transport application areas [10].

ADVANTG provides two computational sequences that generate variance reduction parameters using the CADIS and FW-CADIS [11] methods. The parameters consist of space- and energy-dependent weight-window targets and a biased source that is consistent with the weight map. The primary output from ADVANTG is a WWINP file containing space- and energy dependent weight-
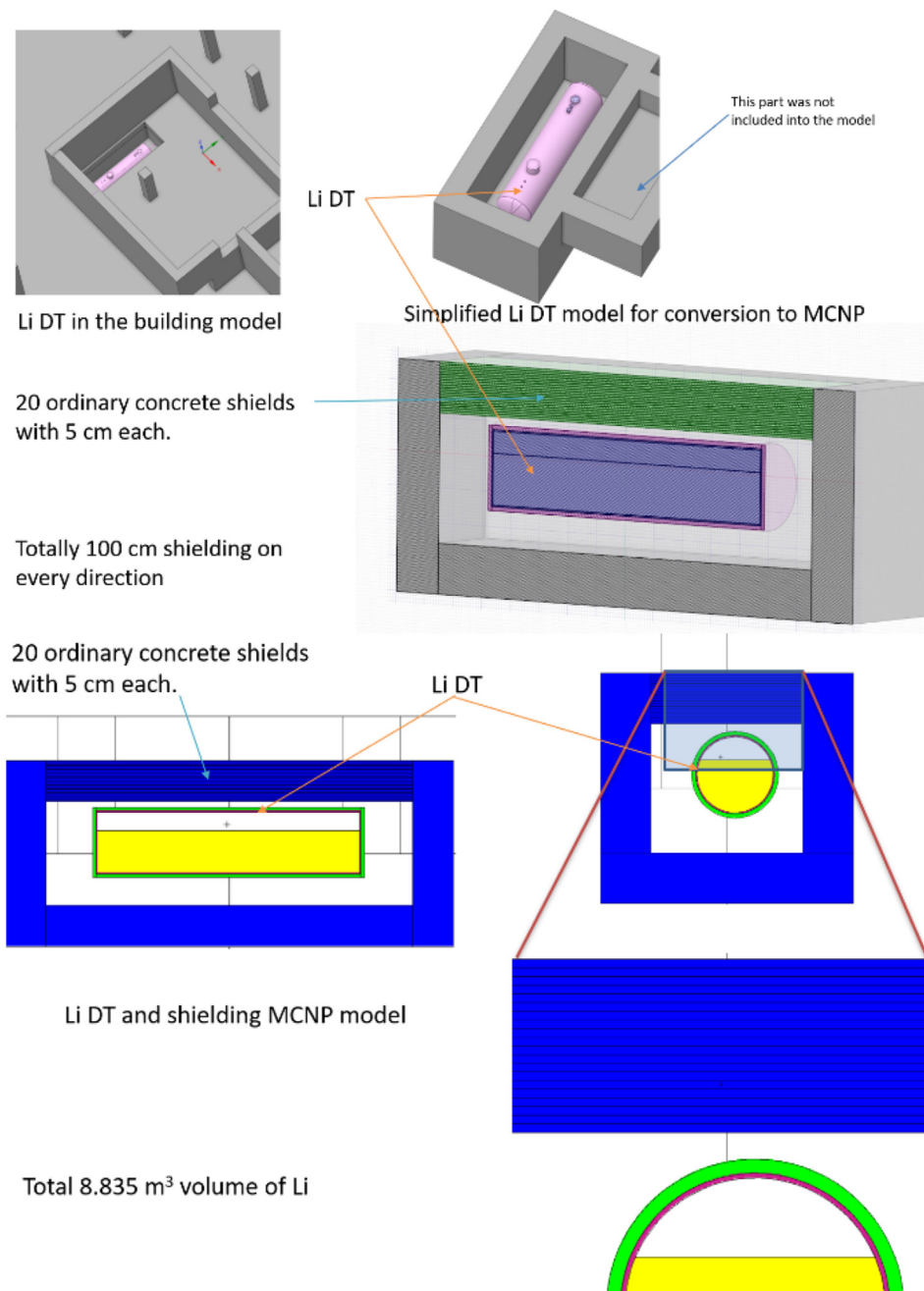
Fig. 4. CAD and MCNP model for DT.

window lower bounds (see Figure 5) and the user's MCNP input file extended with biased source distributions and weight-window control parameters.

Dose rate maps in the Li sampling cell are provided for the cases during the operation of the Li loop, and after shutdown of 0 s for the DT. An MCNP simulation of the DT and Li loop problem was performed using the ADVANTG-generated variance reduction parameters. As with the reference simulation of 1.0e+09 nps, a run-time limit of 860 min was reached in an hour of wall-clock time using 60 threads. In order to reach statistical good results, LEI Computing cluster HPC: SGI Altix ICE8400 consisting of 240 CPU's was employed.

Considering the shielding geometry, it was clear, that WW techniques were needed in both cases. The FW-CADIS variance reduction parameters have a dramatic impact on the mesh tally results for this problem. Relatively uniform statistical uncertainties are obtained throughout the problem. Without variance reduction, only most of the mesh tally voxels outside the DT shielding box have high errors, while with the FW-CADIS variance reduction parameters, the voxels close to possible leakage locations have uncertainties at or below 10% level.

A conventional (i.e. without WW) MCNP simulation would require an extremely long run time to obtain results converged at this level. With ADVANTG, the calculation of the variance reduction parameters and MCNP simulation could be performed on a computer cluster system longer or using more threads in order to give better maps resolution.
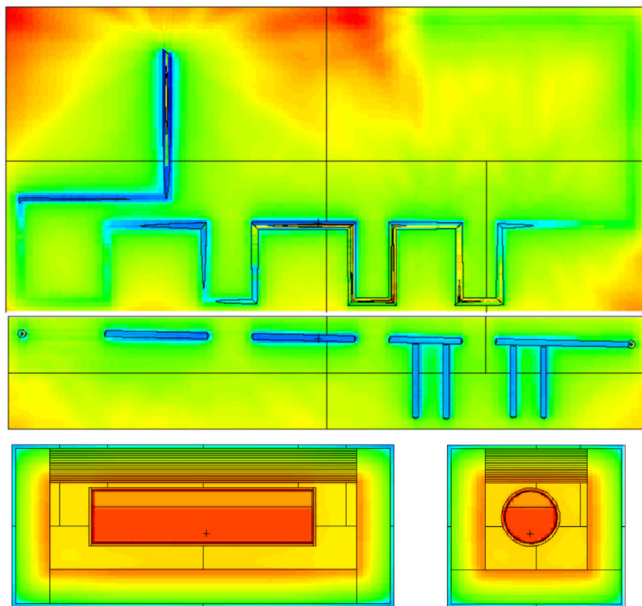
Fig. 5. WW generated by ADVANG for Li pipes in the sampling cell (top) and DT (bottom).

Table 1
Resulted amount of selected ACPs (mg) [12].

	CL	LiHX	TotLi	Tot
^{55}Fe	49.8535	38.0806	10.4030	99.0651
^{54}Mn	0.0000	0.0000	10.2713	10.2713
^{51}Cr	0.0779	0.0606	0.0008	0.1393
^{57}Co	0.4131	0.3761	0.1832	1.0424
^{60}Co	0.8790	0.6843	0.1779	1.7413

3.3. Source specification

The initial source (arising from ACP's) description employing the above-mentioned assumptions are shown in the table below. *CL* denotes the cold leg pipe, whereas *LiHX* denotes the Primary Heat Exchanger. The *TotLi* column displays the total quantity of ACPs dissolved in the Li (sum of the whole loop), whereas the *Tot* column displays the total amount of the given ACP in the entire loop (practically it is the sum of *CL*, *LiHX* and *TotLi* contributions, with small differences coming from small deposits located elsewhere in the Li loop [12].

As can be seen from the table above (see Table 1 for more details), the *CL* has a greater deposit than the *HX* (excluding the ^{54}Mn and generally Mn, which does not saturate at all due to its high solubility in Li). Only the final component (the coldest component of the *HX*) deposits in *HX*, comparable to other Be-7 findings.

Four reactions were considered to be added to the ACPs list: ^{55}Mn $(n,\gamma)^{56}$Mn, ^{58}Ni$(n,p)^{58}$Co, ^{59}Co$(n,\gamma)^{60}$Co and ^{58}Fe $(n,\gamma)^{59}$Fe, which means these new nuclides needed to be tracked in the system: ^{59}Co (as CP from the base materials as well as initial impurities in Li), ^{56}Mn, ^{58}Fe and ^{59}Fe.

The number of materials that can be activated by neutron flux and the cross section of reactions are both factors in neutron activation of nuclides. Every corrosion material in the system, as well as its isotopes, must have their activation determined. We'll need to know about corrosion materials and cross sections for this.

Radiation risks are raised due to the long decay time and strong gammas from ACPs. As it was stated, the most concerned ACPs are
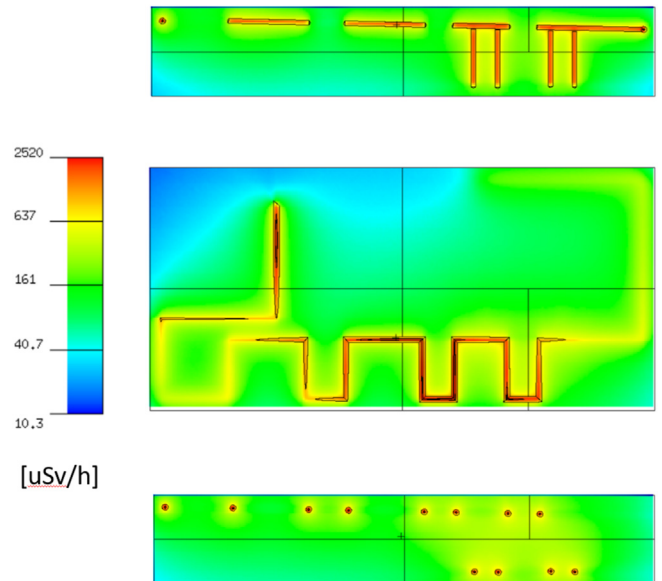

Fig. 6. Dose rate maps for Li loop pipes at different geometrical cross-sections.

^{55}Fe, ^{51}Cr, ^{54}Mn, ^{56}Co, ^{57}Co, ^{60}Co, which are the major emitters following the activation in case of stainless steel (A304 or A316) while is utilized for the loop piping elements. Some of these elements or their derivatives are long-lived isotopes that emit β or γ rays. The source above was used to calculate the dose rate maps of the components (dump tank and Li loop pipes).

4. Dose map calculations

4.1. Impurity Control System

This section presents the gamma dose-rate maps calculations and analysis, which is important in case of supporting the design of the Lithium loop and safety assessment. The simulation results were obtained considering the radiation decay source from Be-7, which is produced by d-Li interaction. It has a half-life of 53 days and emits gamma rays with 477 keV of energy. In addition, the ACP's contribution was evaluated and compared to Be-7 case.

Simulation geometry was Li pipes, where gamma transport calculation was performed. A series of gamma transport are performed using the MCNP Monte Carlo, and radiation maps are provided for maintenance design of the Li Systems. Figure 6 represents ACP's dose-rate map at different geometrical cross sections. It is clear to see, that most part of the radiation remains inside the pipes and higher dose is accumulated in the regions where larger number of pipes are installed. At these particular places, the dose rate can be at 100 μSv/h and it drops down to 20 μSv/h at the distance of 2 m away from the pipe with Lithium inside. It is worth to note, that the statistical error was up to 3%.

In order to have a better understanding of the Be-7 contribution to the total radiation fields around the lithium pipes, the separate MCNP calculation was performed to estimate the difference of the potential hazard from the gammas coming from Be-7 isotope. Figure 7 represents data in graph, where the plotted data is taken from the map along the green arrow in the right-hand side of the picture. Here one can see, that the difference of two cases (Be-7 and ACP's) has a difference by the factor of 200. It is clear, that ACP's plays the most important role in the production of gamma radiation in the Li Sampling Cell environment. It is due to the significant contribution from Mn-54, as it is outlined in the Table 1.

4.2. Dump tank

The DT results section contains radiological field estimation by presenting radiation dose maps with the shielding. The dose rate maps are provided on high resolution mesh grids covering the DT and concrete shielding.

As it was mentioned in Section 3.1 and in Figure 4, the MCNP model was created with multi-layered shielding plate, which allows estimating gamma penetration in the shielding. The shielding plate is a 1 m-thick concrete block, which is subdivided into 20 segments for this study.

MCNP flux tally F4 was employed to calculate gamma flux in each of the segments, while mesh tally was used to generate a dose-rate map inside the DT and in the shielding blocks using the flux-to-dose conversion factor ICRP-74 [13]. Figure 8 presents various maps at different geometrical cross-sections. Moreover, the statistical error was reached no lager that 1 % inside the shielding plates, with 1e9 gamma particle histories.

The same Figure 8 contains a map, with a specific color scale. The radiological area classification scheme according to Council Directive 2013/59/Euratom [14] were applied ($<0.5 \ \mu Sv/h, \ < 3 \ \mu Sv/h, \ < 10 \ \mu Sv/h, \ < 1 \ mSv/h, \ < 100 \ mSv/h, \ \geq 100 \ mSv/h$: white area, blue, green, yellow, orange, red) with the dose rates shown in the same color scheme.

One of the objectives in this study was to estimate the biological dose and identify possible shielding optimization. As mentioned above in the report, two simulation cases were performed in order to see the dose contribution coming from Be-7 and arising from ACPs.

Figure 9 shows this comparison in high fidelity maps. One can see, that considering Be-7, the arbitrary level of 3 μSv/h could be reached with 20 cm thickness of ordinary concrete, while taking into account the radiation coming from ACP's, the block of at least of 50 cm would keep the radiation level safe outside the DT shielding box. It can be concluded, that the suggested design of 1 m thickness of shielding would be more than sufficient to keep the dose rate less than 3 μSv/h. In addition, the simulation shows, that with current design, the radiation level outside the DT shielding box, will be not more than 1e-3 μSv/h.

5. Summary

The shielding analyses presented in this work will be used to assist the design of the Lithium loop and DT as well as the safety assessment. The radiation decay source from Be-7, which is formed through d-Li interaction, is considered in this study. For the safety reasons, radiation shielding simulations have been performed arising from ACPs.

The neutronics geometry for the DT and Lithium loop components, were built. The lithium dump tank and Li Sampling cell were subjected to gamma transport calculations. In the study, the biological dose were presented, and possible shielding optimization were offered and examined in depth. The MCNP Monte Carlo was used to simulate a series of gamma transports, and radiation shielding recommendations are made for the Li system's maintenance design, including DT analysis. Neutron flux and energy distribution for ICS and DT was calculated using ADVANTG generated variance reduction parameters in order to perform subsequent gamma transport calculations.

The components in consideration, namely the lithium DT and ICS pipes from the Li Sampling Cell, were subjected to gamma transport calculations. To this purpose, simulation geometry for the DT and Li loop pipes was generated and shielding analyses were performed to aid in the design of the DT and safety evaluation. In addition, biological dose maps for DT shielding and ICS pipes were provided. The radiation source from Be-7 and ACPs is considered in this report.

For a better understanding of the Be-7 contribution to the total radiation fields around the lithium pipes, a MCNP simulation was run to evaluate the difference in potential impact from Be-7 isotope produced gammas. It can be stated that the difference in contribution between Be-7 and ACPs could be reached by a factor of 100. In the Li Sampling Cell environment, it is obvious that ACPs play the most critical role in the production of gamma radiation. It's because
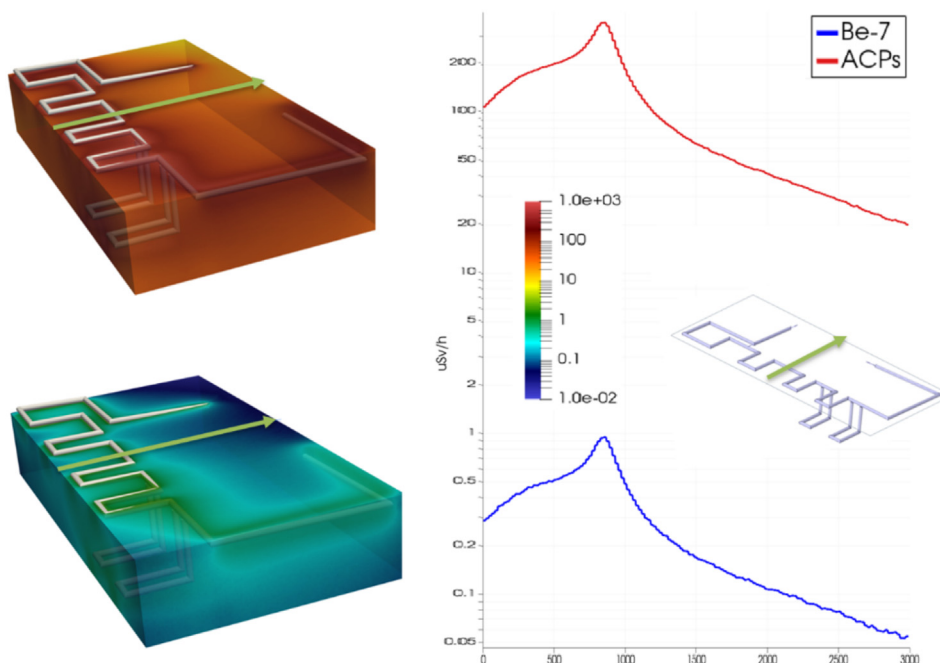

Fig. 7. The trend of dose rate along the arrow for the Li Sampling Cell.
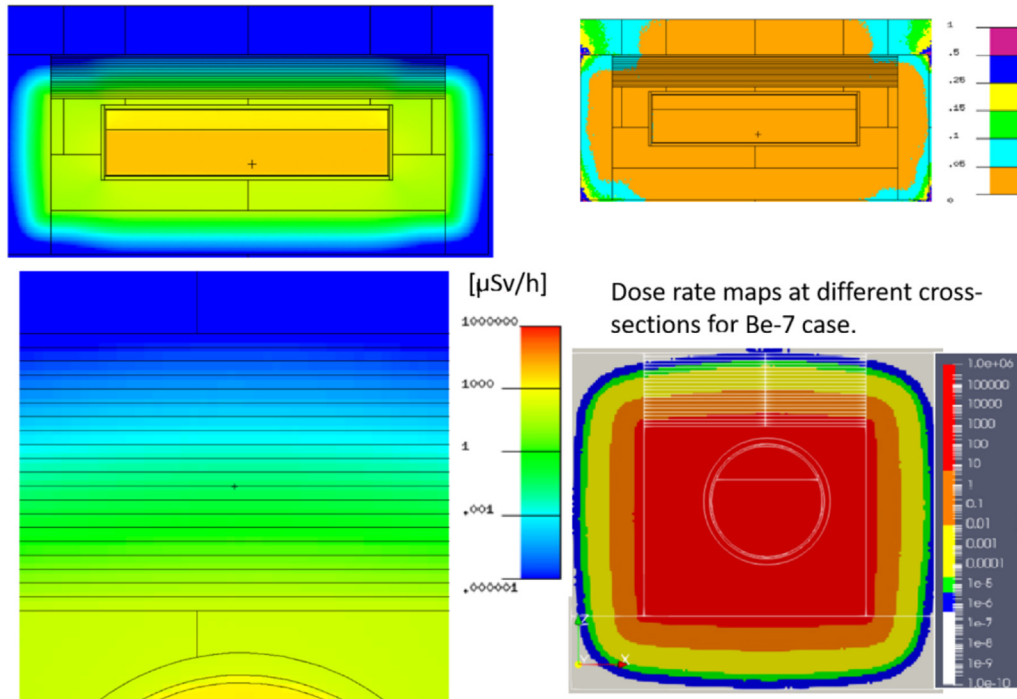
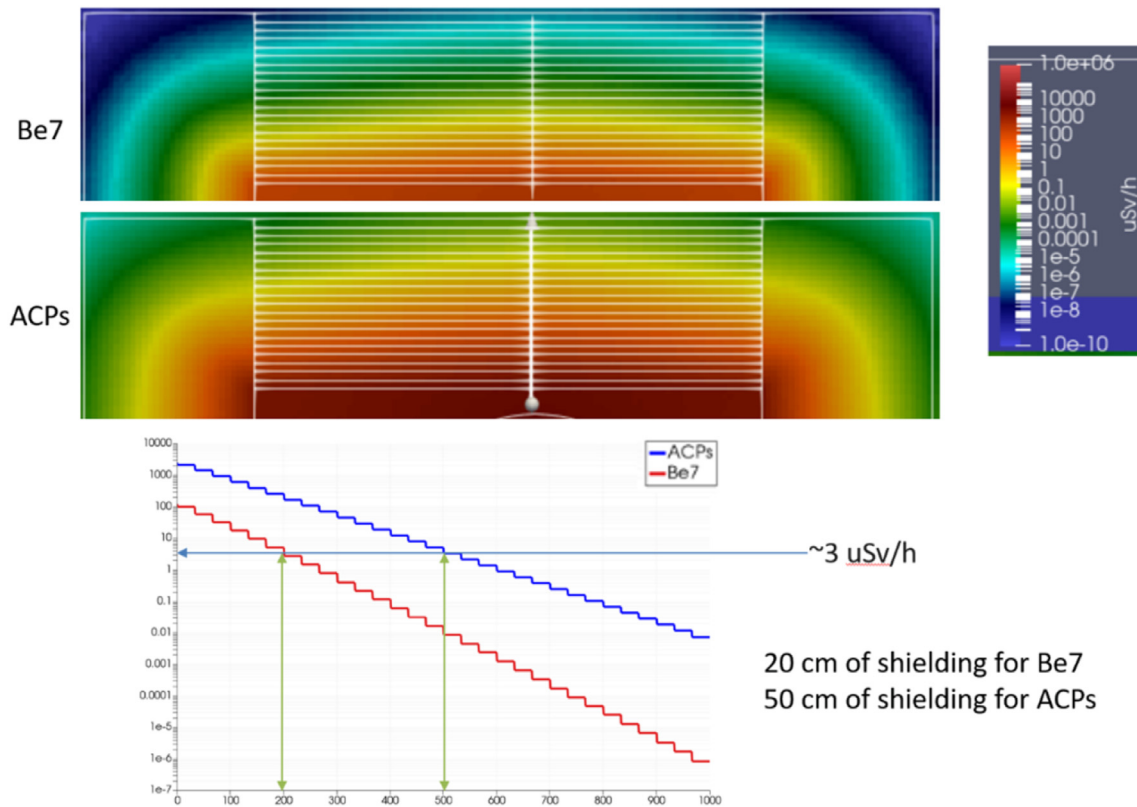Fig. 8. Dose rate maps and statistical error for DT.

Fig. 9. The trend of dose rate along the arrow in DT the shielding plate.

of Mn-54 substantial influence as the most dominant nuclide in the list of ACPs.

In addition, DT shielding analysis reviled, that for the case of Be-7, an arbitrary level of 3 μSv/h could be achieved with standard concrete of 20 cm thickness, while taking into consideration the radiation from ACPs, a block of at least 50 cm would maintain the

radiation level safe outside the DT shielding plate. It was determined that the proposed shielding design of 1 m thickness would be more than enough to maintain the radiation rate below 3 μSv/h. Furthermore, the modeling reveals that the radiation level outside the DT shielding box will be less than 1e-3 μSv/h with the existing design.

Declaration of competing interest

The authors declare that they have no known competing financial interests or personal relationships that could have appeared to influence the work reported in this paper.

Acknowledgments

References

[1] A. Ibarra, A. García, R. Román, M. Pérez, W. Krolas, DONES Plant Description Document", EFDA_D_2MP8HQ, 2021.

[2] C.J. Werner, J.S. Bull, C.J. Solomon, et al., MCNP6.2 Release Notes", LA-UR-18-20808, 2018.

[3] Ulrich Fischer, Barbara Bienkowska, Krzysztof Drozdowicz, Manuela Frisoni, Fernando Mota, Francisco Ogando, Yuefeng Qiu, Gediminas Stankunas, Grzegorz Tracz, Neutronics of the IFMIF-DONES irradiation facility, Fusion Engineering and Design 146 (2019) 1276–1281. Part A.

[4] U. Fischer, C. Bachmann, J.P. Catalan, T. Eade, D. Flammini, M. Gilbert, J.-Ch. Jaboulay, A. Konobeev, D. Leichtle, L. Lu, F. Malouch, F. Moro, P. Pereslavtsev, Y. Qiu, J. Sanz, P. Sauvan, G. Stankunas, A. Travleev, A. Turner, F. Ogando, I. Palermo, R. Villari, Methodological approach for DEMO neutronics in the European PPPT programme: tools, data and analyses, Fusion Engineering and Design 123 (2017) 26–31.

[5] J. Ahrens, B. Geveci, Ch. Law, ParaView: an end-user tool for large-data visualization, in: D. Charles, Hansen, Johnson Chris R (Eds.), Visualization Handbook, Butterworth-Heinemann, 2005, pp. 717–731. ISBN 9780123875822.

[6] L. Lu, U. Fischer, P. Pereslavtsev, Improved algorithms and advanced features of the CAD to MC conversion tool McCad, Fusion Eng. Des. 89 (2014) 1885–1888.

[7] S.W. Mosher, S.R. Johnson, A.M. Bevill, A.M. Ibrahim, C.R. Daily, T.M. Evans, J.C. Wagner, J.O. Johnson, R.E. Grove, ADVANTG—An Automated Variance Reduction Parameter Generator, ORNL/TM-2013/416 Rev. 1, Oak Ridge National Laboratory, Oak Ridge, TN, 2015.

[8] I.E. Stamatelatos, T. Vasilopoulou, P. Georgolopoulou, Neutron streaming along shielding penetrations of high energy medical accelerators using MCNP and ADVANTG codes, Physica Medica 32 (Supplement 3) (2016) 304.

[9] T.M. Evans, A.S. Stafford, R.N. Slaybaugh, K.T. Clarno, Denovo: a new three-dimensional parallel discrete ordinates code in SCALE, Nucl. Technol. 171 (2) (2010) 171–200.

[10] Y. Qiu, U. Fischer, Global flux calculation for IFMIF-DONES test cell using advanced variance reduction technique, Fusion Science and Technology 74 (4) (2018) 406–411.

[11] J.C. Wagner, D.E. Peplow, S.W. Mosher, FW-CADIS method for global and regional variance reduction of Monte Carlo radiation transport calculations, Nucl. Sci. Eng. 176 (1) (Jan. 2014) 37–57.

[12] D. Tamas, Z. Andras, Updates on the Estimation of Generation and Distribution of Impurities in the Li Loop. Technical Note on Subtask ENS-5.3.21-T25-03, Report IDM Ref. No. EFDA_D_2NSUM6, 2021.

[13] ICRP Conversion coefficients for use in radiological protection against external radiation. Publication 74, Annals of the ICRP 26/3 (1997).

[14] Council Directive 2013/59/Euratom of 5 December 2013 Laying Down Basic Safety Standards for Protection against the Dangers Arising from Exposure to Ionising Radiation, and Repealing Directives 89/618/Euratom, 90/641/Euratom, 96/29/Euratom, 97/43/Euratom and 2003/122/EuratomOff L13, EU document, 2014, pp. 1–73 [Online]. Available: https://eur-lex.europa.eu/eli/dir/2013/59/oj.